Recent developments in two fundamental aspects of electron backscatter diffraction

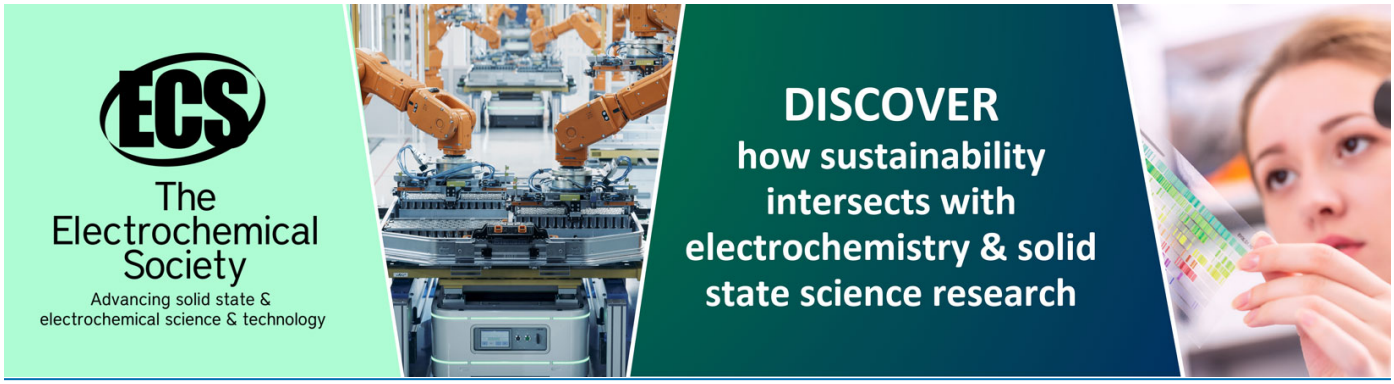

IOP Conf. Series: Materials Science and Engineering **55** (2014) 012011 doi:10.1088/1757-899X/55/1/012011

Recent developments in two fundamental aspects of electron backscatter diffraction

K P Mingard[1], A P Day[2] and P N Quested[1]

[1] National Physical Laboratory, Hampton Road, Teddington TW11 0LW, Great Britain
[2] Aunt Daisy Scientific, Claremont House, Lydney GL15 5DX, Great Britain

E-mail: ken.mingard@npl.co.uk

Abstract. Two very different aspects of electron backscatter diffraction (EBSD) are considered in this paper. Firstly, the use of the technique for the measurement of grain size is discussed with particular reference to the development of international standards to help ensure reproducible and repeatable measurements. In particular the lessons learnt for both calibration of the complete SEM-EBSD system and in choice of the correct data acquisition and processing parameters from an international round robin are summarized. Secondly, extending the capability of EBSD through development of new detectors is discussed. New shadow casting methods provide a means to achieve better accuracy in definition of sample-pattern geometry, while increased detail can be obtained by larger cameras and ultimately direct electron detection.

1. Introduction

A full review of the entire state of the art in electron backscatter diffraction (EBSD) would be impossible in a short article so it is intended here to look at a two particular aspects of EBSD, one being an application of the technique in common use and the other a development of the technique through possible improvements to detector technology.

One of the most common and important applications of EBSD is the measurement of grain size and phase, particularly for industrial quality control and materials characterisation. This is because of its capability to not only group pixels of one particular orientation, but also to unambiguously define grain boundaries by the misorientation across a boundary. Both enable software routines to automatically calculate sizes based on area or linear intercept. However, this automation brings with it the usual risk of accepting any number produced without understanding the factors which affect the accuracy of the result. The first section will review a recent study [1] of the repeatability and reproducibility of this fundamental measurement and ways of improving it through, for example, international standardisation [2, 3].

Advances in EBSD detector technology have been evolutionary rather than revolutionary in the past decade. Acquisition rates are one of the most commonly quoted parameters for a detector, and the maximum rates have increased perhaps by a factor of 10 over 10 years, with quoted maxima of between 600 and 700 patterns per second. At such rates the drive for faster detectors is perhaps lessening and other factors are beginning to receive attention such as accuracy and detail possible in acquisition of electron backscatter patterns (EBSPs). This includes the possibility of moving from current phosphor/CCD cameras to direct electron detection.

2. Measurement of grain size by EBSD

Studies comparing the results of grain size measurements by optical and EBSD methods have been carried out over the past 15 years [4-10], but reported comparisons of measurements by different laboratories have been few [11, 12] and are old enough that they do not reflect improvements in EBSD detectors software and scanning electron microscopes of the past 10 years. In some of these works differences were observed in grain size between optical and EBSD and besides the greater spatial resolution of EBSD technique other factors were noted, such as limitations of optical methods in detecting boundaries below a certain misorientation and the variable effectiveness of etching in different samples affecting optical measurements.

More recently, an interlaboratory comparison was carried out in support of a new international standard, ISO 13067 "Microbeam analysis - Electron backscatter diffraction - Measurement of grain size and Ddstribution" [2] to provide uncertainty data for grain size measurement by EBSD. Commercially pure (CP) titanium metal bar with an average grain size of approximately 30 μm was chosen to produce uniform and repeatable samples since, in addition to being suitable for the EBSD technique, this size would allow comparison with optical microscopy methods of grain size measurement such as ASTM E112 [13]. The following is a summary of the full report of this round robin [1]. The report also includes details of the studies undertaken prior to the round robin to confirm the consistency of the grain size in the central region of all the samples used. In this paper, the phrase "mean grain size" refers to the most commonly used number average mean: there is not room in this paper to discuss the advantages and disadvantages of using various methods of weighted averages based for example on grain size area, nor the advantages of using the full grain size distribution rather than a single value, but these issues are discussed further in reference [1].

Figure 1 summarizes the data for the mean equivalent circle diameter grain size, D_{circle}, as returned from 12 laboratories, each denoted by a letter. Each laboratory measured two samples but in some cases the laboratories measured the two samples with two different microscopes and EBSD systems or in one case with two magnifications; in these cases two sets of two values are shown. It should also be noted that laboratories A and F measured the same sets of samples; similarly the samples measured by C were then measured by H, and those measured by E were measured by L. The mean value of these raw results before removal of any outliers or corrections for errors was 33.7 μm.

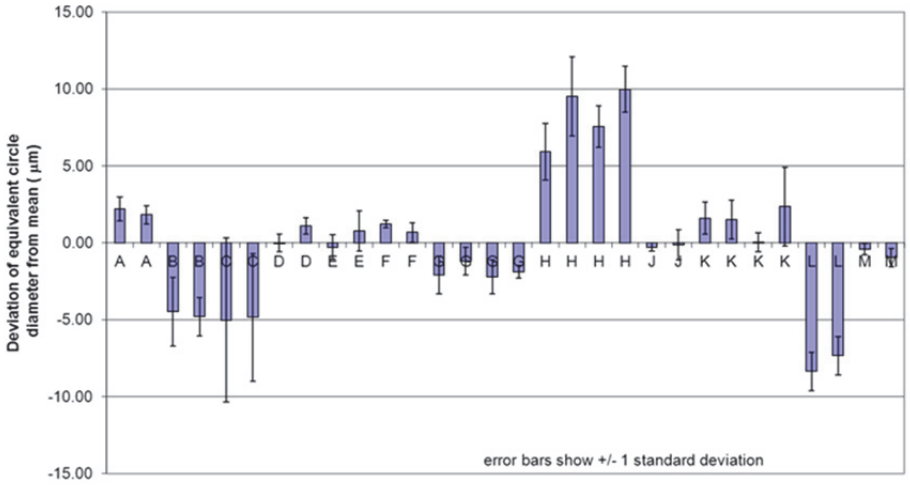

Figure 1. Mean values of D_{circle} for each sample as initially reported by the participants (before any corrections). Values are plotted as the difference from the mean of 33.7 μm. Error bars show ±1 standard deviation from 5 maps contributing to the mean.

Laboratories were informed of their results and were allowed to recheck their results where they appeared to have produced outliers. In two cases errors (discussed later) were identified which enabled some recalculations, after which all the results were analysed statistically following the procedures outlined in, for example, ISO 5725-2 [14, 15]. This analysis resulted in two sets of results being classed statistically as outliers (for reasons also described later) and after excluding these values, the final results of the round robin are summarized in Table 1.

Table 1. Summary of results after statistical analysis

		Equivalent circle diameter D_{circle}	Linear intercept D_{lin}
Overall mean (μm)		33.5	30.1
Repeatability standard deviation (μm)	s_r	0.88	0.74
Reproducibility standard deviation (μm)	s_R	1.98	1.15
Repeatability limit (μm)	r	2.46	2.07
Reproducibility limit (μm)	R	5.55	3.22
Number of measurements after removal of outliers		12	11

The repeatability and reproducibility limits are the values less than or equal to which the absolute difference between two test results obtained under repeatability/reproducibility conditions may be expected to be with a probability of 95 %.

2.1. Analysis of the variability of grain size measurements

Before exclusion of any outliers the mean value of D_{circle} was 33.7 μm but with a spread (± 2σ) of ±8.6 μm. This wide spread was attributed largely to significantly different values reported by just 4 of the laboratories, B, C, H and L, which if completely excluded changed the mean value slightly (34.0 μm), but reduced the spread significantly to ±2.9 μm (± 2σ). Examining the causes of variation for the 4 laboratories B, C, H and L helped identify some of the principal causes for much of the variation.

2.1.1. Magnification. Calibration of magnification was found to be a cause of variation for two laboratories (H and L). In one case this could be corrected, after tracing the problem to linking calibration of the SEM to the EBSD software. This type of software communication can easily occur without the user being aware of it as magnification is all too often taken as an absolute value for the SEM when it should refer only to the size at which the scanned image is displayed. It cannot be emphasized enough that what should be checked is the equivalence of scale bar markings or total image widths on the SEM and EBSD systems, not the magnification!

2.1.2. Step size and sample size. All but one laboratory used a step size of between 2 and 3 μm, or 6 to 9 % of the mean, agreeing well with the empirical rule established by Humphreys [5], that step sizes approximately 10 % of the mean grain size should produce good maps of most microstructures. The one laboratory that used a finer step size of 1 μm obtained a much smaller mean size 15 % below the mean. While this step size allowed resolution of small grains that might have been missed by coarser step sizes, the more important factor was that, for a given set of acquisition conditions and mapped area, acquisition would take 4 or 9 times longer than with, respectively, 2 or 3 μm step sizes, so

instead much smaller areas were mapped. This not only reduced the total number of grains but also eliminated many of the larger grains from the analysis because such grains are more likely to touch the map edges and thus be discarded because they are incompletely analysed.

It is also worth noting that analysing the results from many of the laboratories by plotting running averages showed that, at least for this material, a minimum of between 200 and 300 grains is sufficient to obtain a stable average that will change little as further grains are measured. This is probably applicable to most materials with an equi-axed grain structure and a similar size distribution, but with this quantity of data a cumulative size distribution curve itself could be plotted to give a more comprehensive description of the grain structure.

2.1.3. Specification of minimum grain size. It recommended in the standard ISO 13067 that grains >10 pixels in area will give valid results since EBSD validates each pixel in a grain by measuring its orientation. Pixellation errors, which alter the true grain size at small sizes, are approximately 5 % at the 10 pixel area level. This cut off limit also agrees approximately with conventional image analysis where the minimum size of an object is 9 (3x3) pixels for a square grid or 7 for a hexagonal grid to avoid erosion of step size 1 deleting an object completely. Thus any grain comprised of <10 pixels should be ignored in any calculation because it is unlikely to be well defined in size: this size is called the cut off limit.

In the round robin however a variety of cut off limits were used. Most were stated in terms of pixels although a couple were in terms of a minimum size in micrometres. The cut offs selected by the participants included > 1, 4, 5, 6 or 8 pixels, but most chose 10 pixels. Because of the variation in step sizes chosen, the actual sizes of the cut off limits varied from 2 µm to 10.75 µm, equivalent to 3.46 µm^2 to 91 µm^2. Figure 2 plots the mean grain size against the cut off limit used (where this was known). The cut off is plotted in micrometres rather than pixels to take into account the step size used as well as the number of pixels and suggests that the mean size initially increases before beginning to plateau as the cut off is increased.

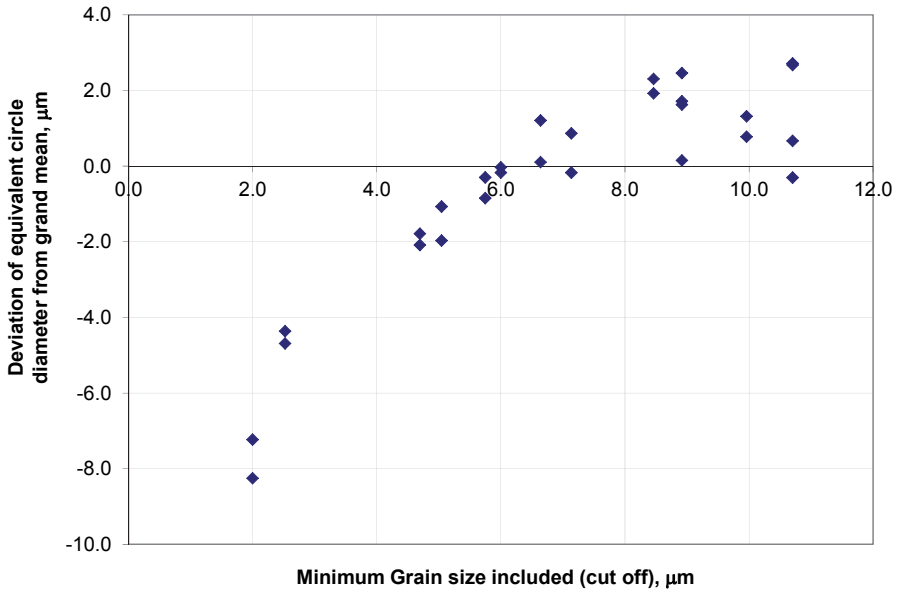

Figure 2. Mean values of D_{circle} for each sample (calculated as the difference from the overall mean value) plotted against the cut off minimum grain size (expressed in µm, not pixels) used by each participant in the calculation of their sample mean size.

The data supplied by individual laboratories was reanalysed to give a clearer idea of the effects of varying the cut off limit. This showed that if a single cut off value, specified in terms of micrometres

rather than pixels, of 8 µm was used for all laboratories (with the exception of the outliers), the data spread in figure 3 was reduced from ≈ 5 µm to 2 µm. It should be noted that good agreement would be achieved at any given cut off above about 8 µm, as long as a single consistent cut off is applied to all the data.

2.1.4. "Clean-up" of map data. A difficult area to specify in the standard ISO 13067 was the amount of data "cleaning", or replacing poorly indexed pixels by more appropriate orientations that might be allowed, since many factors can affect how much and where the poor indexing occurs. Poor data cleaning (or noise reduction) did account for one of the initial outliers (C) in figure 1, and the full report [1] gives more detail than there is room for here about clean-up issues, but it may be noted that the maps in figure 3 show the extremes of the percentages indexed in the raw maps supplied (98.8 and 75 %) and both these maps with suitable clean up produced grain size values very close to the overall mean. One factor in this was the choice of a suitable cut off since this can remove most or all of the poorly indexed pixels. However, if too large a cut off is chosen before data cleaning, subsequent reindexing of the removed pixels may lead to overestimation of the remaining grains.

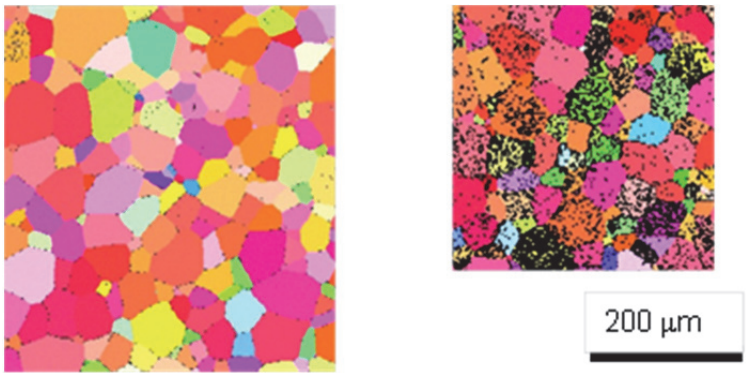

Figure 3. Raw EBSD orientation maps before noise reduction showing two extreme levels of good indexing (left – 98.8 %, right, 75.0 %) which gave very similar mean grain size measurements (34.2 µm and 34.7 µm respectively).

2.1.5. Other factors. A range of other factors can influence the mean grain size value. These include errors in acquisition, two of which can combine to affect the magnification calibration in the vertical direction: firstly, inaccurate measurement of the tilt angle of the specimen, and secondly, drift of the specimen/imaged area which usually occurs in the same direction. Other factors include definitions used such as the chosen value of angular misorientation used to define a grain boundary. In some combinations the effect of these factors can cancel each other out, but if combined to, say, all increase the mean they can add 15 - 20 % to the quoted value.

2.2. Linear intercept and optical grain size measurements

The results discussed in the preceding sections were all based on the use of circle equivalent diameter grain sizes D_{circle}, but linear intercept measurements D_{lin} are also commonly used, particularly when comparing with optical methods of measurement or where grains are not equi-axed. The participants in the round robin were all asked to report D_{lin} as well and these are summarized in Table 1 next to the D_{circle} values, from which it can be seen that:

i) Comparing the overall mean values, the D_{circle} value is about 9 % greater than D_{lin}, which is close to the ratio suggested in the appendix to ISO 13067 [2].
ii) The repeatability of the two measurements is very similar (r_{circle} = 2.54 is 20 % greater than r_{lin} = 2.13), but the reproducibility of D_{lin} is much better than that of D_{circle} (R_{circle} = 5.79 is 70 % greater than R_{lin} = 3.36).

It was also noted that only one laboratory reported linear intercept measurements in both X and Y directions and the same laboratory was the only one to explicitly report using a cut off for minimum linear intercept size in the same way as a cut off value was reported for the equivalent circle diameter. One possible reason for the increased reproducibility range for the D_{circle} measurements is the unassessed error of measurement in the Y direction caused by drift and/or tilt errors which would only be revealed by comparison of D_{lin} measurements in both directions after using this same method to check that the material was truly equi-axed.

Linear intercept measurements were also made on optical images taken from one of the samples. This produced a mean value of 34.6 µm taken from 431 measurements. The good agreement with the EBSD measurements could be seen from plots of the size distribution (figure 4) to be in part a consequence of choosing a suitable cut off value for the minimum grain size chosen for EBSD such that it had a similar effective resolution to that of the optical microscope.

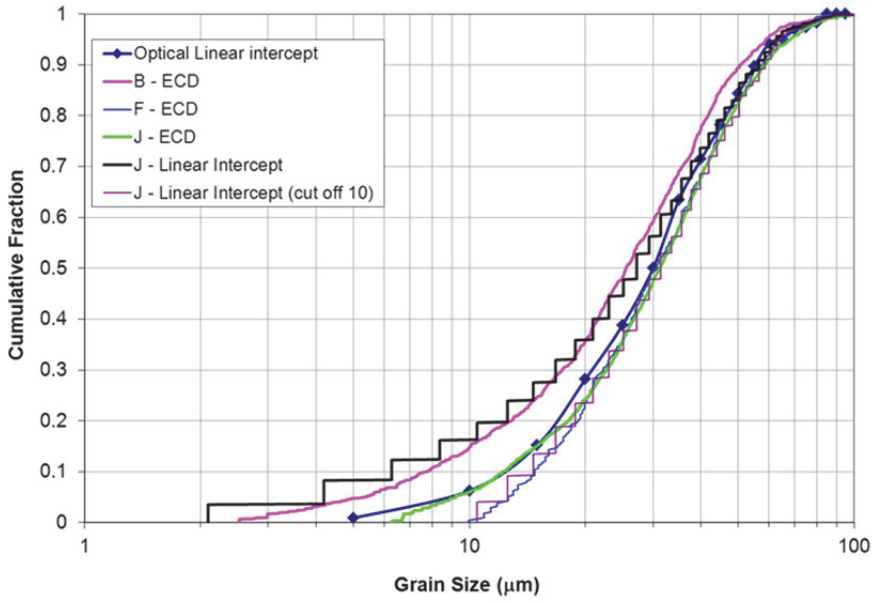

Figure 4. Distribution of optically measured linear intercepts compared with EBSD measurements by linear intercept and equivalent circle diameter from a selection of participating laboratories B, F and J.

2.3. Summary

The use of EBSD for measurement of grain size is now a widely used method in industry and academia and the round robin study described has shown reproducible measurements are possible, but only with careful attention to detail. Even obvious issues such as magnification calibration need to be checked in orthogonal directions and use should be made of both circle equivalent and linear intercept measurements to look for errors caused by, for example, tilt or drift. Use of agreed standards such as ISO 13067 will help with this, and for specific materials attention must be paid to agreeing definitions of grain boundary angles and particularly a minimum grain size (cut off value) used in the calculation. Further studies, extending perhaps to finer grain sized materials, would be useful to establish if greater reproducibility is possible by application of the findings from the current work.

3. EBSD cameras

It was noted in the introduction that acquisition rates have increased by a factor of about 10 in the past decade. However, increased speeds usually require the compromise of a large reduction in the information available from the EBSPs. For much day to day mapping of microstructures this is perfectly acceptable, but there are some applications where high detail and accuracy in EBSP

acquisition is of more importance than speed. Examples of such applications include discrimination between phases with similar structures or small differences in lattice parameter such as tetragonal lead zirconium titanate piezoelectric materials with differences between a and b lattice parameters of < 3 % [16, 17].

A significant application which requires high accuracy and detail in acquired EBSPs is the measurement of strain: a paper by Wilkinson [18] this series will describe this method in more detail, but it is appropriate here to describe some of the implications this has for detector design and accuracy of EBSP acquisition. A key requirement for the measurement of elastic strain is the ability to compare (by cross-correlation) an EBSP from the strained material to an EBSP produced from unstrained material of the same orientation [19]. This can be difficult, if not impossible in, for example, small grained materials in which unstrained positions in each grain may not be identifiable. A way of overcoming this problem is to use a simulated strain free EBSP. This has two main requirements: obviously a method for producing a detailed simulation is needed, but also an accurate knowledge of the geometry of the EBSD system, relating the position of the beam on the specimen generating the EBSP precisely to the position of the camera phosphor and any distortions in the optical path between the phosphor and the CCD camera.

Considering pattern simulation first, there are two possible methods with very different requirements for computational time. Kinematical simulations can produce simple patterns (as shown in figure 5) relatively quickly but studies by Britton [20] have shown that their use can result in significant errors in calculations of strain because of the large differences in intensities, especially at the zone axes of the patterns. Dynamical simulation of EBSPs, pioneered by Winkelmann [21], produces much greater detail, as can be seen in figure 5b. With appropriate filtering of the cross-correlation between the real and dynamical simulations in figures 5a and b, realistic calculations of strain fields can be achieved.

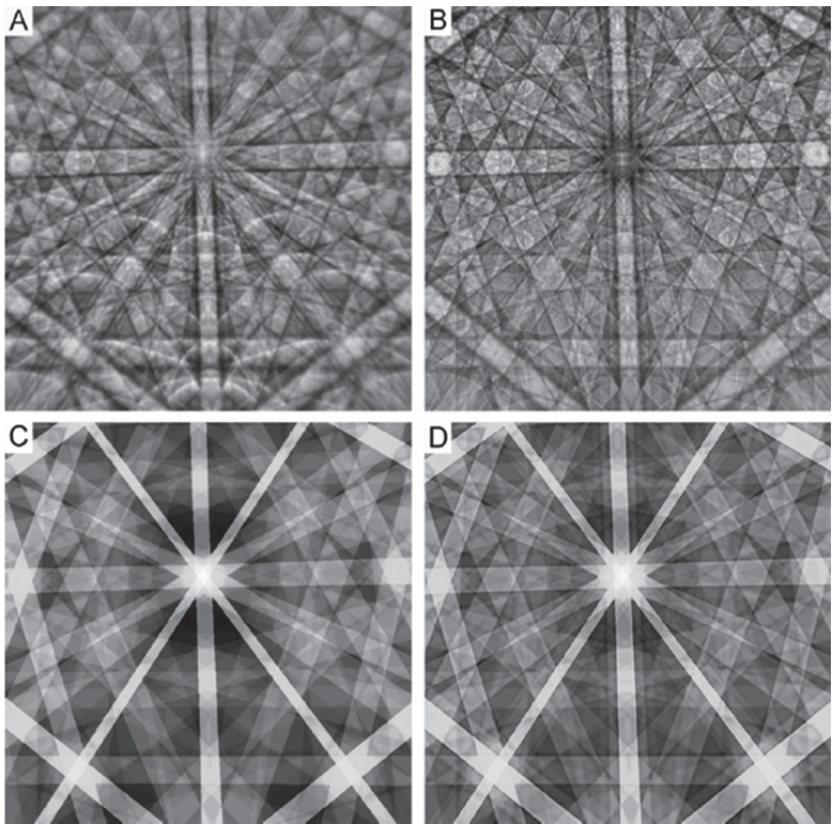

Figure 5. Cropped 20 kV EBSPs from Ge: a) experimental; b) dynamic simulation of pattern with minimum plane spacing of 0.5 Å and no inelastic scattering anistropy; c) Bragg simulation with 204 reflectors and no higher orders; d) improved Bragg simulation with simple band profile and higher order reflectors (after Britton *et al.* [19]).

3.1. Detector development

Given the detail possible from dynamical simulations, it is appropriate to consider if greater detail could be captured with improvements to EBSD detectors. Commercial detectors designed for higher quality pattern acquisition use CCD cameras with 12-bit acquisition and ranging from 1000 to 1600 pixels in their maximum dimension (although in most day to day operations they would be run with binning of pixels to reduce acquisition time and images generally stored after background correction in 8-bit grey scale). An experimental system with a 5 MPixel 16-bit CCD camera with 2448x2050 pixels and a 50 % larger phosphor screen has been demonstrated [22] and figure 6 compares the output of this camera with that of a commercial camera producing 1340x1024 pixel image when positioned 30 % closer. With only static background correction and no averaging, the greater detail, particularly in the black deficiency lines is obvious, as is the greater field of view. The ring and disc shadows visible in the 4 corners of the image will be discussed in the following section.

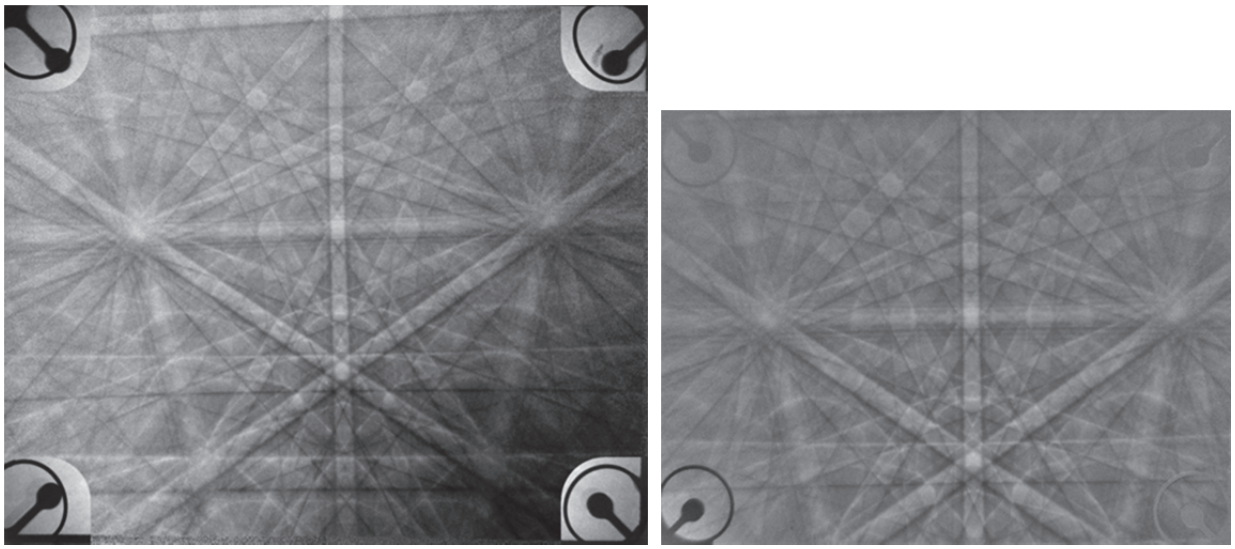

Figure 6. a) 2448 x 2050 pixel EBSP single frame image acquired from a <001> oriented silicon specimen, shown at the same magnification as b) a 1340x1024 pixel image (averaged over 10 frames) from a commercial camera positioned 30 % closer to the specimen.

An alternative method being investigated is to eliminate the phosphor screen and CCD camera altogether and detect electrons directly; previous work has looked at direct electron detection for transmission [23, 24] and low-energy electron microscopes[25] but is now looking at energies suitable for scanning electron microscopy [26, 27]. The conversion by the phosphor screen of the electrons to light and then reconversion of this light back to electrons by the CCD is obviously inefficient. Detecting the electrons directly increases the signal available and can in principle run faster with greater definition in the pattern as well. It also reduces errors arising from misalignment of the optic system and, being planar, removes distortions due to the lens, both of which cause problems for comparison of real and simulated patterns [28, 29]. Figure 7 shows an EBSD pattern from a GaN thin film acquired with a direct electron detection Timepix chip positioned approximately 3 cm in front of the sample [26]. The EBSD pattern shown in figure 7 was acquired at an acceleration voltage of 30 kV, at a beam current of order 0.5 nA, a beam spot size of around 2 nm and an acquisition time of 1 second. While the field of view is limited, the increase in detail available with this camera is noticeable.

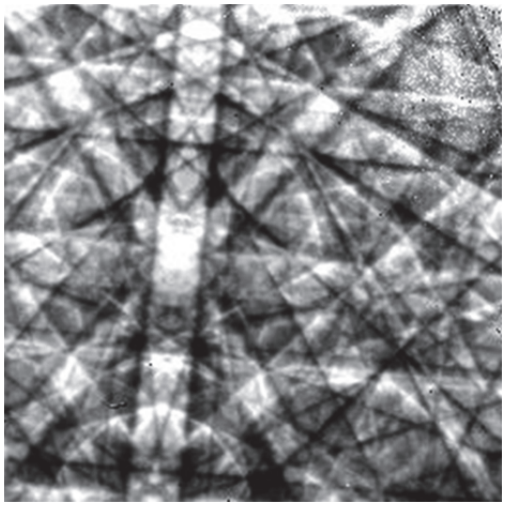

Figure 7. Direct electron detection EBSP of GaN acquired with a Timepix chip at 30 kV (after Vespucci *et al.* [26]).

3.2. EBSD camera geometry and pattern centre measurement

It has been shown [29] that, while not obvious in day to day use, detector geometry issues such as optic axis misalignment, spherical distortion by the EBSD system lens and vignetting can be significant and need to be minimized to reduce the effects that simulation must take into account. The 5 MPixel camera used to produce the pattern shown in figure 6 was designed to minimize these effects, for example selecting the camera lens to produce minimum spherical distortion even with the large apertures needed to increase light levels. Using the methods described in [29], these issues were accurately characterized since they would remain generally constant in operation. The other major design factor was to increase the rigidity of the system while allowing for fine adjustments to centre the system at precisely the required working distance before fixing in place. Even with this rigidity, the specimen-camera geometry, described by the pattern centre (PC) parameter, still needs to be measured accurately for each new specimen, and to do this a shadow casting technique was used [29]. With the geometry shown in figure 8, the solid discs projecting from a brass grid mounted in front of the camera phosphor produce shadows on the phosphor. Having assembled the front small grid in alignment with a larger grid mounted in the plane of the phosphor, the whole system of grids, specimen and camera can be aligned so that the common axis of the two grids marks the pattern centre when the circular disk artefacts are aligned with the rings. Even when the system is out of alignment, the true pattern centre can be calculated from the displacement of the disks relative to the circles.

Figure 9a shows an EBSP from a silicon specimen acquired with the 5 MPixel camera in which superimposed on the disc shadows are simulations of these discs produced using the calculated pattern centre parameters. To demonstrate the tracking of the movement of the pattern centre, the sample was displaced in the Z-direction by +0.30 mm, in X by 0.52 mm and Y by 0.24 mm. Figures 9b and c show enlargements of the disc shadows and simulations before and after the movement. At the centre between the four disc shadows the position of the pattern centre calculated from the disc positions is shown by the large "X" relative to the perfect alignment with the camera axis denoted by the smaller "+". It can be seen the "X" tracks the movement of the vertical {220} band from the EBSP with the change in PC caused by the sample displacement, indicating the calculations must be at least close to an accurate value. It may be noted that there is scope for refinement of this calculation as the ellipse fitting used to simulate the disc shadows could still be improved.

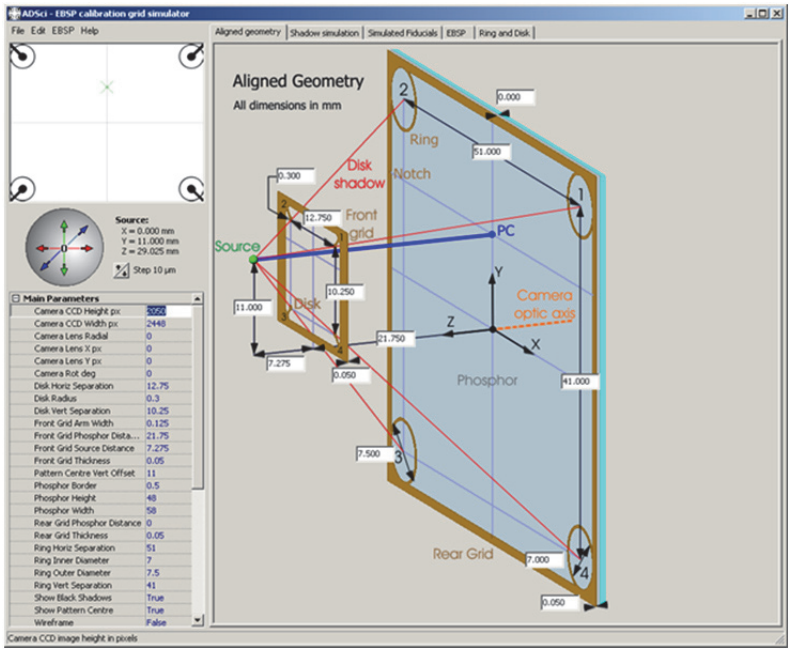

Figure 8. Geometry of shadow casting system

a)

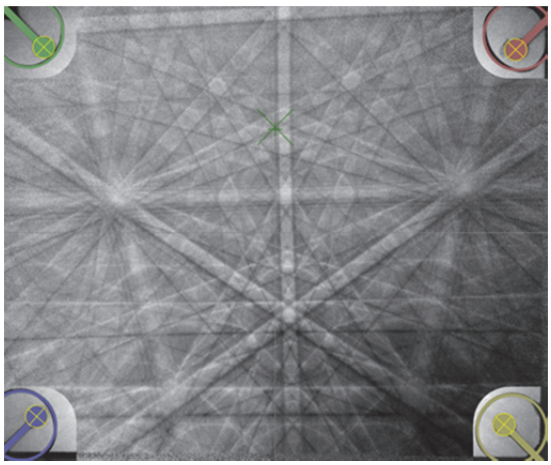

b)

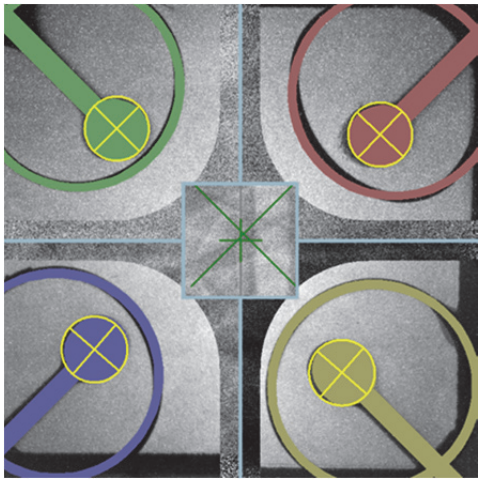

c)

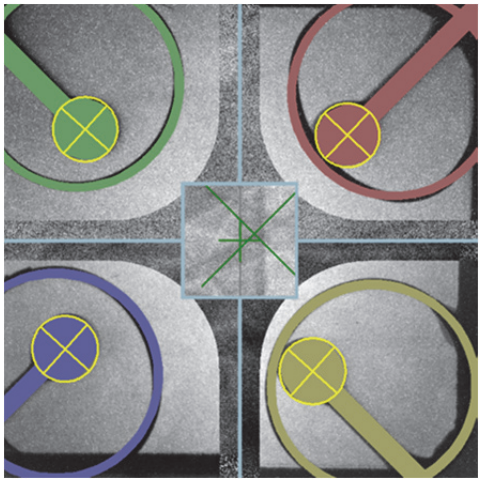

Figure 9. Calculation of pattern centre shown by simulation of disc shadows. a) Full pattern with disc shadows seen in corners; b and c) Show enlargements of the disc shadows and simulations before and after movement of the sample by +0.30 mm in Z, 0.52 mm in X and 0.24 mm in Y. Position of the pattern centre indicated by green X, tracking the movement of the dark vertical {220} band.

4. Conclusions

EBSD technology is now sufficiently advanced that grain size measurement by this method for development and quality purposes in industry is becoming important. However care needs to be taken in both calibration of the complete SEM-EBSD system and in choice of the correct data acquisition and processing parameters. Development of international standards provides guidance to minimize errors.

Extending the capability of EBSD to enable more widespread use of, for example, the local measurement of strain requires improvements in the accuracy and detail available in EBSP acquisition. New shadow casting methods provide one way to achieve better accuracy in definition of sample-pattern geometry while increased detail can be obtained by larger cameras and ultimately direct electron detection.

Acknowledgements

Funding for organizing the work at the National Physical Laboratory was provided by the UK Government Department for Business, Innovation and Skills. The willing participants from five continents in the grain size round robin are gratefully acknowledged as is the assistance of Graham Sims and Stuart Saunders in setting up the VAMAS TWA 37 to oversee the work.

References

[1] Mingard K P, Quested P N and Peck M S 2012 *NPL Report MAT56*; ISSN 1754-2979 (London: National Physical Laboratory)
[2] ISO 13067: *Microbeam analysis - Electron backscatter diffraction - Measurement of average grain size*. (Geneva: International Standards Organisation)
[3] ASTM E2627-10: *Standard practice for determining average grain size using electron backscatter diffraction (EBSD in) fully recrystallized polycrystalline materials*. (West Conshohocken, PA: ASTM International)
[4] Gao N, Wang S C; Ubhi H S and Starink A 2005 *J. Mat. Sci. Lett.* **40** 4971-4974
[5] Humphreys F 1998 *J. Microsc.* **195** 170-185
[6] Day A P and Quested T E 1999 *J. Microsc.* **195** 186-196
[7] Bowles A, Dargusch M, Davidson C, Griffiths J and Nogita K 2004 *Mater. Trans.* **45** 3114-3119
[8] Piazolo S, Sursaeva V G and Prior D J 2005 in: *Proc. 14th Int. Conf. Textures of Materials - ICOTOM 14*. (Leuven, Belgium)
[9] Lins J F C, Sandim H R Z, Ribeiro R B and Pinto A L 2003 *Acta Microsc.* **12** 121-124
[10] Wright S 2010 *Prakt. Metallogr.* **47** 1
[11] Randle V 2003 *Pilot interlaboratory exercise for comparative EBSD measurements*. (Swansea: University of Wales)
[12] Ryde L 2004 *Report no.: IM-2004-121*; ISRN: SIMR/R- -04/080- -SE ISSN: 1403-848X
[13] ASTM E112-96: *Standard test methods for determining average grain size*. (West Conshohocken, PA: ASTM International)
[14] ASTM International Standard E691-09: *Standard practice for conducting an interlaboratory study to determine the precision of a test method*. (West Conshohocken, PA: ASTM International)
[15] BS ISO 5725-2: 1994: *Accuracy trueness and precision of measurement methods and results - Part 2: Basic method for the determination of repeatability and reproducibility of the standard measurement method*. (London: British Standards Institute)
[16] Farooq M U, Villarrutia R, MacLaren I, Kungl H, Hoffmann M J, Fundenberger J-J and Bouzy E 2008 *J. Microsc.* **230** 445-454
[17] Burnett T L, Comyn T P, Merson E and Mingard K P 2008 *IEEE Trans. Ultrasonics Ferroelectrics And Frequency Control* **55** 957-962

[18] Wilkinson A J, Britton T B, Jiang J and Karamched P S 2014 *IOP Conf. Ser.: Mat. Sci. Engng.* **55** 012020
[19] Wilkinson A J, Meaden G and Dingley D J 2006 *Ultramicroscopy* **106** 307-313
[20] Britton T B, Maurice C, Fortunier R, Driver J H, Day A P, Meaden G, Dingley D J, Mingard K and Wilkinson A J 2010 *Ultramicroscopy* **110** 1443-1453
[21] Winkelmann A, Trager-Cowan C, Sweeney F, Day A P and Parbrook P 2007 *Ultramicroscopy* **107** 414-421
[22] Mingard K, Day A, Quested P and England G 2011 in: *RMS EBSD Conference*. (Dusseldorf)
[23] Roberts P T E, Chapman J N and MacLeod A M 1982 *Ultramicroscopy* **8** 385-396
[24] Moldovan B J G, Nomerotski A and Kirkland A 2009 *Nucl. Inst. Meth. Phys. Res. A* **604** 108-110
[25] Sikharulidze I, van Gastel R, Schramm S, Abrahams J P, Poelsema B, Tromp R M and van der Molen S J 2011 *Nucl. Inst. Meth. Phys. Res. A* **633** Suppl. 1, S239-S242
[26] Vespucci S, Kumar N, Edwards P R, Maneuski D, O'Shea V, Day A, Mingard K and Trager-Cowan C 2013 in: *RMS EBSD Conference*. (Oxford)
[27] Wilkinson A, Molodovan G, Britton, T, Bewick, A, Clough R and Kirkland A 2013 *Phys. Rev. Lett.* **111** 065506
[28] Villert S, Maurice C, Wyon C and Fortunier R 2009 *J. Microsc.* **233** 290-301
[29] Mingard K, Day A, Maurice C and Quested P 2011 *Ultramicroscopy* **111** 320-329